JMEPEG (2017) 26:5553–5562
DOI: 10.1007/s11665-017-2955-5

1059-9495/$19.00

Laser Nitriding of the Newly Developed Ti-20Nb-13Zr at.% Biomaterial Alloy to Enhance Its Mechanical and Corrosion Properties in Simulated Body Fluid

M.A. Hussein, A. Madhan Kumar, Bekir S. Yilbas, and N. Al-Aqeeli

(Submitted May 3, 2017; in revised form August 7, 2017; published online October 11, 2017)

Despite the widespread application of Ti alloy in the biomedical field, surface treatments are typically applied to improve its resistance to corrosion and wear. A newly developed biomedical Ti-20Nb-13Zr at.% alloy (TNZ) was laser-treated in nitrogen environment to improve its surface characteristics with corrosion protection performance. Surface modification of the alloy by laser was performed through a Nd:YAG laser. The structural and surface morphological alterations in the laser nitrided layer were investigated by XRD and a FE-SEM. The mechanical properties have been evaluated using nanoindentation for laser nitride and as-received samples. The corrosion protection behavior was estimated using electrochemical corrosion analysis in a physiological medium (SBF). The obtained results revealed the production of a dense and compact film of TiN fine grains (micro-/nanosize) with 9.1 µm below the surface. The mechanical assessment results indicated an improvement in the modulus of elasticity, hardness, and resistance of the formed TiN layer to plastic deformation. The electrochemical analysis exhibited that the surface protection performance of the laser nitrided TNZ substrates in the SBF could be considerably enhanced compared to that of the as-received alloy due to the presence of fine grains in the TiN layer resulting from laser nitriding. Furthermore, the untreated and treated Ti-20Nb-13Zr alloy exhibited higher corrosion resistance than the CpTi and Ti6Al4V commercial alloys. The improvements in the surface hardness and corrosion properties of Ti alloy in a simulated body obtained using laser nitriding make this approach a suitable candidate for enhancing the properties of biomaterials.

Keywords biomaterial, corrosion, laser treatment, simulated body fluid, titanium alloy

1. Introduction

Titanium (Ti) and its alloy have been commonly utilized in several biomedical fields, for example orthopedics, implants, and dentistry, due to their preferred biocompatibility and higher resistance to corrosion (Ref 1, 2). However, Ti implants fail due to the reduced resistance to wear, and corrosion (Ref 3, 4), which causes the creation of wear debris. Wear debris may cause an inflammatory reaction and result in an implant loss due to osteolysis (Ref 5-7). Therefore, various types of surface modifications and surface treatments have been applied to enhance the surface structure, composition, resistance to wear and corrosion (Ref 4), and biocompatibility (Ref 8).

Laser surface modification, physical vapor deposition (PVD), chemical coating have been used to improve the wear resistance of Ti alloy (Ref 9-12). Plasma ion implantation, laser melting, laser alloying, laser nitriding (Ref 13, 14), laser etching, laser cladding, thermal spray, plasma spray, and electrochemical treatment were used successfully to improve hardness and corrosion properties of biomaterials (Ref 15, 16). Although plating and plasma spraying showed the formation of a hard layer, the applied coating showed less bonding strength with Ti substrate (Ref 17). Plasma ion implantation showed higher adhesion; however, the obtained too small thickness (tens of nm) limits their applications (Ref 18). Plasma spray was reported to apply an HA coating on Ti. Although it is low-cost and offers rapid deposition, the coating showed the low adhesion strength and cracks (Ref 19). Plasma surface alloying has been applied to deposit Ti-B nanopowders on Ti substrate which showed improvement in the in vitro cytocompatibility (Ref 20). TiN, TiC coating has been prepared on different alloys using ion plating; these films show high resistance to wear and high hardness (Ref 21-23).The nitriding was reported to be an effective way to improve the tribological properties of Ti alloy (Ref 24) due to the high solubility of nitrogen in Ti, the strengthen occurs by solid solution strengthen of the nitrogen to form a TiN layer on the top layer of the substrate (Ref 25). Nitriding may be obtained by ion beam nitriding (Ref 26) and laser gas nitriding (Ref 26, 27).

There has been considerable interest in improving the surface characteristics of Ti alloy in recent years through the development of a TiN layer on the surface (Ref 28). A TiN layer possesses greater hardness than a Ti layer, which enhances the corrosion and mechanical properties of the alloy (Ref 28). A TiN layer has been shown to be biocompatible (Ref 8, 29) as well as physically and chemically stable (Ref 30).

M.A. Hussein, Center of Research Excellence in Corrosion, Research Institute, King Fahd University of Petroleum and Minerals (KFUPM), Dhahran 31261, Saudi Arabia and Department of Mechanical Engineering, Kafrelsheikh University, Kafrelsheikh 33516, Egypt; **A. Madhan Kumar**, Center of Research Excellence in Corrosion, Research Institute, King Fahd University of Petroleum and Minerals (KFUPM), Dhahran 31261, Saudi Arabia; **Bekir S. Yilbas** and **N. Al-Aqeeli**, Department of Mechanical Engineering, King Fahd University of Petroleum and Minerals (KFUPM), Dhahran 31261, Saudi Arabia. Contact e-mail: naqeeli@kfupm.edu.sa.

Different techniques for depositing a TiN layer on the surface have been reported in the literature, including physical vapor deposition (PVD), chemical vapor deposition (CVD) (Ref 31, 32), plasma nitride (Ref 33), ion implantation (Ref 34), and laser nitriding (Ref 29). However, the investigations indicated that an ion-implanted layer of Ti6Al4V was removed after a few years (Ref 35). PVD was successfully used to form TiN with higher corrosion resistance; however, it exhibited a low bonding strength. Plasma nitriding was reported to reduce the corrosion resistance (Ref 36). A TiN layer formed by either CVD or PVD exhibited greater hardness; however, it also exhibited a low bonding strength. Among these techniques, laser nitriding is considered effective in terms of its short time requirements, its flexibility, its controlling structure, its composition, and the dimensions of the processed zone (Ref 36). Laser nitriding exhibited better bonding and interfacial properties with the substrate than ion implantation, CVD, and PVD (Ref 37, 38).

Many researches have conducted studies on improving tribological and anti-corrosion performance of Ti-6Al-4V using laser nitriding (Ref 39-42). However, due to the toxic effects of Al and V (Ref 2), significant effort has been dedicated to the development of a nontoxic alloy made of biocompatible elements. The novel nanostructured Ti20Nb13Zr alloy was recently developed (Ref 43). TiNbZr exhibited potential in the biomedical field and is considered a superior alternative to biomedical grade Ti-6Al-4V (Ref 41). However, Ti alloy exhibited lower resistance to corrosion and wear (Ref 4, 44); thus, the surface and corrosion properties of this alloy must be enhanced to enable its use in bioimplants. Few studies have focused on the laser nitriding of TiNbZr alloy. Laser nitriding has already been adopted to enhance the corrosion protection performance of Ti-13Nb-13Zr and TiNbZrTa alloys (Ref 28, 45).

In the current work, we aimed to examine the impact of laser nitriding on the corrosion protection and surface characteristic of a newly developed TNZ alloy. The microstructure and morphology were investigated by monitoring x-ray diffraction (XRD) pattern and field emission scanning electron microscopy (FE-SEM). The mechanical properties were assessed by nanoindentation measurements. The corrosion behavior of the treated and untreated TNZ substrates in simulated body fluid (SBF) was characterized by potentiodynamic polarization (PDP) and electrochemical impedance spectroscopy (EIS) measurements.

2. Experimental Work

2.1 Laser Nitriding and Characterization

The alloy accommodated in this work is newly developed near-β Ti-20Nb-13Zr at.% (TNZ) alloy fabricated by ball milling and spark plasma sintering (Ref 43). A sample having a 4 mm thickness and 20 mm diameter was used in the study. Laser nitriding was implemented using a CO_2 laser (LC-ALPHAIII) with a moderate output control of 2 kW. During the laser treatment process, nitrogen gas was continually purged and was coaxially purged with the beam of the laser. Figure 1 displays a diagram of the laser nitriding process of the TNZ alloy surface. The several tests based on the parametric investigations were carried out to select the optimum laser processing parameters. The optimum laser parameters were assessed incorporating the criteria for the crack-free, cavity-free, and regular laser scan tracks without excessive melt flow at the treated workpiece surfaces. In this case, increasing laser output power by 10% more than the selected value results in deep cavity formation at the surface while reducing by 10% gives rise to solid heating at the surface. Similar arguments can also apply for the laser scanning velocity, which results in small changes in the scanning velocity (7% less or more), shallow depth melting or surface morphology with deep cavities. The laser nitriding parameters are presented in Table 1. Preliminary observations of the surface of the nitrided samples were made by optical microscopy. XRD (a Bruker AXSD8 machine with Cu-Kα radiation, 40 kV and 30 mA) was used to study the present phases in the as-fabricated and nitride samples. FE-SEM (Tescan Lyra 3) was used to investigate the microstructure and morphology of the untreated and treated alloys.

2.2 Mechanical Testing

To evaluate the mechanical performance, Young's modulus and hardness of the untreated and nitride samples were measured using nanoindentation test. The nanoindenter tester (CSM Instruments SA, Switzerland) was used at room temperature. A loading and unloading rate of 60 mN/min with a maximum load of 500 mN was applied with a pause time of 10 s using the diamond four-sided pyramid Vickers indenter. A load–displacement plot based on Oliver WC, Pharr was adopted to calculate the Young's modulus and hardness of the alloys from nanoindentation software (Ref 46).

2.3 Preparation of the SBF

Corrosion studies were conducted in SBF solution. The SBF (pH 7.4, 1 L) was prepared with an ionic concentration equivalent to that of human body plasma according to previously reported procedure (Ref 47).

2.4 Electrochemical Corrosion Measurements

The electrochemical corrosion of the as-received and laser nitrided TNZ alloy substrates was assessed via PDP and EIS tests in SBF medium. The electrochemical corrosion tests were measured using a classic three-electrode cell assembly, realized by fitting a tubular tube on top of the TNZ substrates with an exposed area of 19.6 mm^2. The electrochemical cell was driven with a potentiostat (Gamry 3000) and Echem analysis software. Further, the material to be tested acted as the working electrode, and a saturated calomel electrode (SCE) and a graphite rod performed as the reference and auxiliary electrodes, respectively. Prior to each electrochemical experiment, open circuit potential (OCP) was monitored for 1 h in the SBF to attain the stable value. EIS was performed at sweeping frequencies downward from 105 to 0.01 Hz, monitoring 10 points per decade. Potentiodynamic polarization testing was performed by scanning the potential from −0.250 to 1.5 V at a scan rate of 0.5 mV/s. For comparison purposes, commercially available alloys, such as CpTi and Ti6Al4V, were also used under same conditions.

3. Results and Discussion

3.1 Structural and Microstructural Investigations

In order to achieve the laser nitride surface without melting, laser treatments were carefully performed using optimized

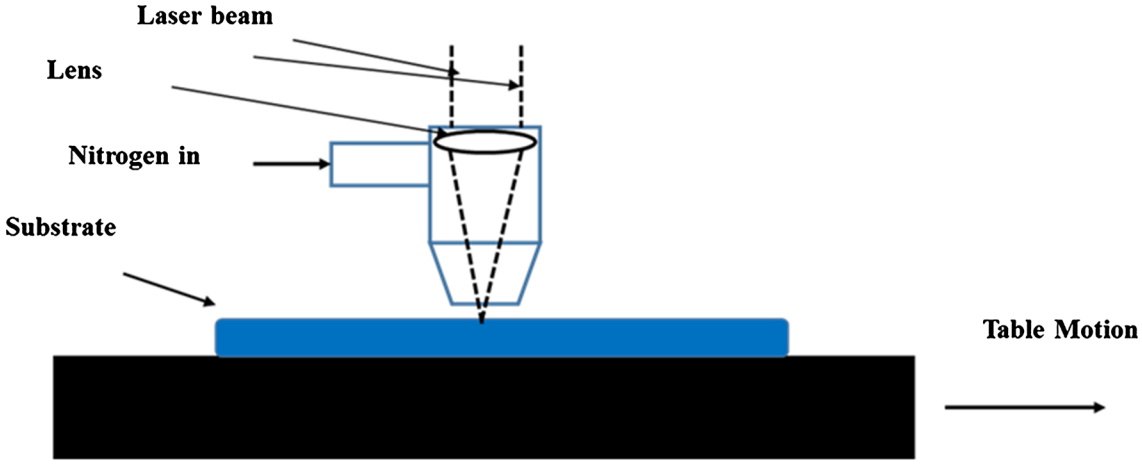

Fig. 1 Experimental laser nitriding setup

Table 1 Laser nitriding processing parameters

Scanning speed cm/s	Power, W	Frequency, Hz	Nozzle gap, mm	Nozzle diameter, mm	Focus setting, mm	N_2 pressure, kPa
10	1	1500	1.5	1	27	600

parameters. The nitride sample surface exhibits a golden-yellowish color (Fig. 2a), revealing the production of a TiN layer on the alloy (Ref 41). The XRD pattern of the as-received and nitrided samples indicates the presence of a high-intensity β phase and an α phase, confirming that the β phase is dominant compared to the α phase (Fig. 2b). As clear from XRD pattern, closer to 30°-50° area, no oxide peaks are observed. The main phase is TiN phase along with the main β TiNbZr phase (β Ti will be used for simplification) in the nitride layer. The small α peak is observed for the treated sample. The treated sample exhibits clear peaks for the TiN (FCC) phase as indexed in (Fig. 2b). The peaks of untreated Ti20N13Z alloy showed high intensity of β Ti phase at (110) and (211) due to the existence of high amount of β stabilizer element (20 at.%Nb) in the base alloy. The intensity of β phase reduced after laser nitriding which might attribute to the TiN (FCC) formation on the surface. The incoherence between β Ti(BCC) and the newly formed TiN (FCC) in the surface might be the reason for the reduction in the intensity of β Ti phase after laser nitriding (Ref 45). The formation of a TiN phase was accompanied by a decrease in the β phase peak which was also reported by another researcher (Ref 41).The TiN formation is attributed to the diffusion of nitrogen from the surface to form an interstitial solution Ti(N) which forms a compound of Ti and N after saturation and with continues supply of nitrogen forms a TiN layer on the surface (Ref 48). According to the equation: Ti $\rightarrow$ -Ti(N) $\rightarrow$ Ti2 N $\rightarrow$ TiN (Ref 48).

The nitrogen diffuses in the substrate forming a solid solution (interstitial) in α Ti phase (Ref 49). After exceeding the concentration limit of nitrogen in αTi, a new TiN (FCC) phase will be formed.

It is also noticed from XRD pattern (Fig. 2b) that the main peak of β Ti phase (110) was shifted to left direction after nitriding indicating an increase in lattice parameter due to the formation of solid solution of Ti with nitrogen (Ref 50). Lattice parameter increased from 0.33 to 0.3339 nm after laser nitriding. It was observed that the TiN peak showed broadening related to the obtained fine structure (nano-/micrograined as shown in Fig. 3(b, c).

An FE-SEM micrograph of the laser-treated cross section is presented in Fig. 3. The results show that the microstructure of the base alloy is a β-Ti (BCC) matrix (whiter areas in the micrograph) surrounded by a α-Ti (HCP) region (darker areas in the micrograph), which confirms the XRD results. The back-scattered electron (BSE) image indicated that the average thickness of the laser nitride was approximately 9.1 µm below the surface (Fig. 3a). The micrograph of laser-treated samples indicated the formation of a micro-/nanostructure as shown in BSE image (Fig. 3b, c). A close examination of the treated layer revealed that it does not exhibit major cracks due to the dense and compact structure with fine grains formed over the surface layer (Fig. 3b, c).

3.2 Nanoindentation Measurements

Figure 4 displays the load–displacement curves for the untreated and treated alloys at a maximum load of 500 mN. Extracted parameters related to the wear resistance, Young's modulus, and a hardness value of the material are presented in Table 2. The curve of the laser nitrided sample is shifted to the left compared to that of the untreated sample (Fig. 4), possibly due to the compressive residual stress because of the fabrication of the TiN phase with thermal quenching (Ref 51). Further, Young's modulus of the laser-treated sample also increased to 199.7 GPa, compared to 129 GPa for the untreated sample, owing to the laser surface nitriding. From the literature (Ref 52), Young's modulus of the titanium nitride surface was identified to change between 100 and 600 GPa depending on the deposition parameters and the technique used (Ref 52). Hardness measurements from the nanoindentation indicated that the laser treatment enhanced the surface microhardness of the sample. The HV of the treated sample was 13.68 GPa, whereas that of the untreated sample was 7.62 GPa. This enhancement in the hardness value is associated with the construction of a hard TiN ceramic layer over TNZ surface. The

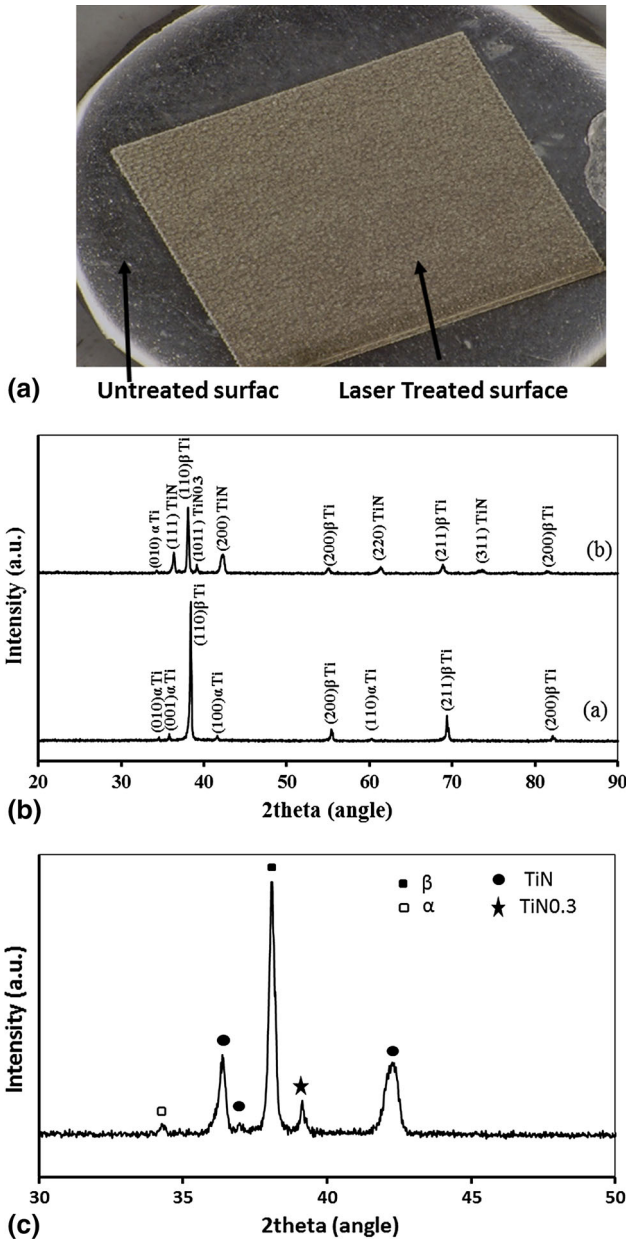

Fig. 2 Laser nitride and as-received samples: (a) optical image of the surface, (b) XRD pattern of an as-received sample and treated sample, (c) XRD pattern of treated sample closer to 30°-50° area

increased hardness will contribute to enhancing the resistance of alloy surface to the wear and will help prevent the formation of incompatible wear debris that loosens the implant and hence increasing the life span of the biomaterials (Ref 4). The coating resistance to plastic deformation was evaluated by H^3/E_r^2 using the extracted nanoindentation information (Ref 53, 54). The increase in hardness due to the formation of the nitride layer on the surface contributed to enhancing the resistance of the material surface to plastic deformation and, thus, wear (Ref 55). As shown in Table 3, the developed Ti20Nb13Zr at.% alloy exhibited a greater hardness value than Ti-6Al-4V alloy, and the H^3/Er^2 value of the treated alloy surface (0.075) was higher than that of the untreated sample (0.0269), which indicates that the treated alloy possesses a higher wear resistance and

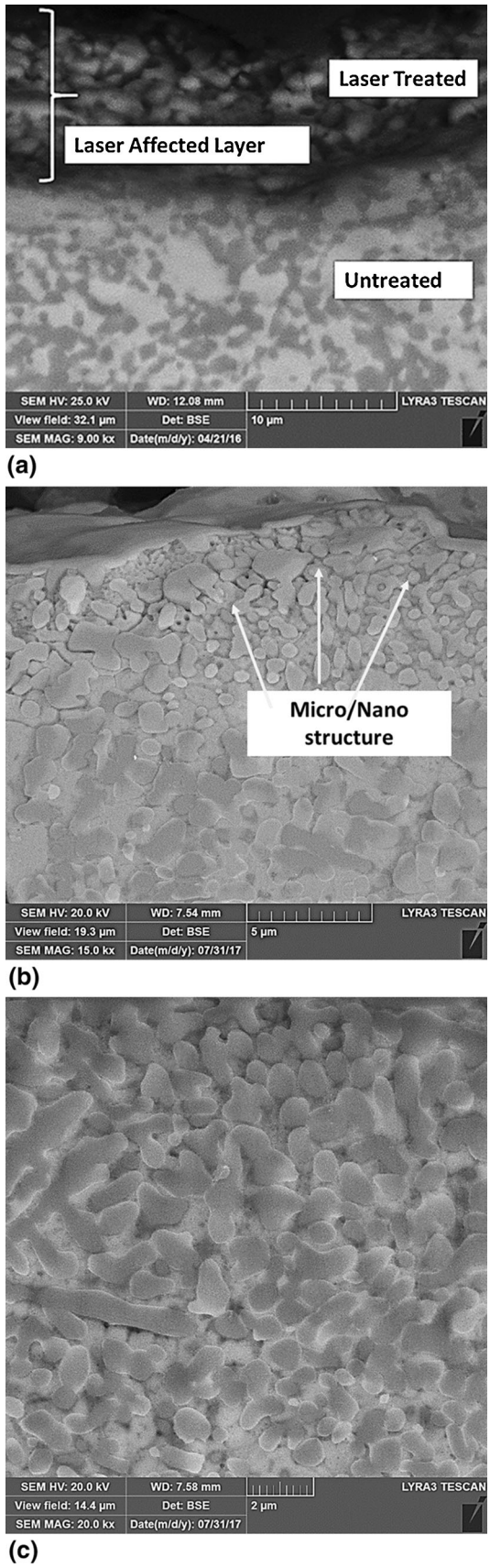

Fig. 3 FE-SEM micrograph of the laser-treated sample: (a) base alloy with laser-affected layer; (b) and (c) micro-/nano-sized grains

toughness than the untreated sample. The treated sample was approximately three times more than the untreated sample. The same results were also obtained by Ng et al. (Ref 45), as shown in Table 2. These improvements in hardness and thus in wear resistance are due to the formation of a ceramic TiN layer due to the reaction of N_2 with Ti alloy and the formation of a harder ceramic layer of TiN. The increase in hardness due to the presence of TiN as a result of laser nitriding was also observed for Ti6Al4V alloy (Ref 37). The nano-/microstructure refinement observed after laser nitriding may be also contributed to the enhancement of hardness of surface layer. This is in accordance with a well-known Hall–Petch relation that states the increase in hardness and yield strength correlated with a decrease in the grain size (Ref 43, 56). The modification in metallurgy after laser nitriding of Ti20Nb13Zr alloy, such as surface microstructure, surface hardness, and grain size, will improve the wear resistance.

Ti-6Al-4V has been used for biomedical applications. However, V and Al may be toxic (Ref 2); thus, the selection of alloying elements is important in designing the alloy to meet the biomaterial characteristics, particularly its biocompatibility. TNZ could be an alternative to Ti-6Al-4V. The structure, surface morphology, surface hardness, and corrosion properties of the base alloy surface have been improved via laser nitriding; thus, laser nitriding could be a good tool for enhancing the characteristics of biomaterials and thus increasing their longevity and service life.

3.3 Electrochemical Corrosion Studies

PDP results for the bare and laser nitrided TNZ substrates are displayed in Fig. 5. The measured and calculated Tafel parameters, such as corrosion potential (E_{corr}), corrosion current density (i_{corr}), Tafel slopes, and the corrosion rate, are summarized in Table 3. The anodic polarization curves for bare TNZ, Ti64, and Cp Ti imply the distinctive stimulating polarization from −0.35 V up to 0.15 V, exhibiting a straight increase in the corrosion current density with the potential. Subsequently, variations in breakdown and repassivation with increasing potential occurred, after which the substrate transitions into an entirely passive area in which the corrosion current density remains constant. By contrast, laser-treated TNZ substrates rapidly passivated and continued a lower current density with the investigated anodic region. Further, the slope of the anodic branch was comparatively small, and the polarization phenomenon occurred gradually. This behavior

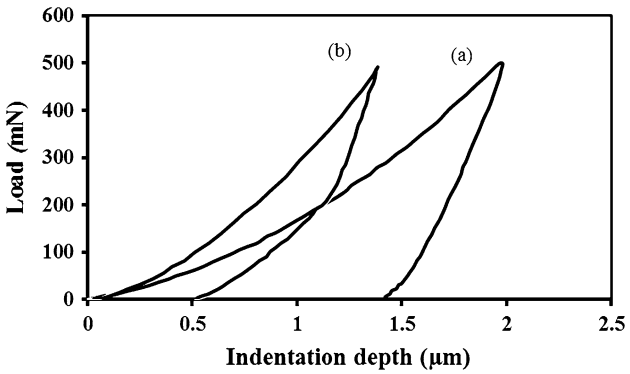

Fig. 4 Load–displacement curves of (a) treated and (b) untreated alloys

proves that laser-treated TNZ substrates exhibit less polarization in anodic regions, revealing an improved corrosion-resistant performance in the SBF medium. Overall, the corrosion performance of the laser-treated substrates was comparatively nobler than that of the as-received substrates because TiN surface is chemically inert than titanium (Ref 57-59).

In addition, the corrosion current density is an important factor in predicting the surface protection of materials against corrosion, as it is in inverse proportionate to the corrosion rate. Hence, the materials typically exhibit a superior surface-protective performance while exhibiting the lowest corrosion current density (Ref 60). The i_{corr} values of the substrates can be arranged in the following order: laser-treated TNZ < bare TNZ < Ti6Al4V < CpTi. The lower i_{corr} value of the laser-treated TNZ is attributed to the improved surface microstructure with the existence of a noble TiN phase inside the nitrided film (Ref 41).

The reason for the observed variation might be related to the nature of surface film that forms on the surface of cp Ti and Ti alloys in SBF medium. In addition, the stronger and the more stable, continuous, tightly adherent TiO_2 passive film on the Ti-based implant alloys, the better the corrosion resistance and also the lesser the release of the metal ions from the alloys. In general, Ti6Al4V is an alpha–beta titanium alloy, where Al and V act as stabilizers of α and β phases, respectively, modifying the Ti transformation temperature; this temperature is about $980 \pm 20\ ^{\circ}C$, and the alloy may present two different microstructures: globular and lamellar, which provide mechanical and corrosion resistance to the Ti alloy (Ref 61, 62). Different structural morphologies may be transferred to or may have influence on the surface layers of the alloy, which could lead to enhanced corrosion resistance with different biological behaviors from those of unmodified Ti substrates. The presence of strong passivating elements like Al, V, Nb, Zr in sufficient amounts and their uniform distribution can also be probable reasons for the superior corrosion resistance exhibited by this alloy in SBF. It has been reported that modification of passive TiO_2 layer by the addition of α and β alloying elements reduces Cl^- ingress into the oxide layer, thereby improving the structural integrity of the oxide film such that pit initiation events were reduced (Ref 63). Moreover, the obtained results were in good agreement with the previous works (Ref 64-67). The same trend of results was also reported (Ref 68); Ti-xNb-13Zr alloys were more corrosion resistant than both Ti and Ti-6Al-4V in Ringer's solution, as the passivating film formed on Ti-xNb-13Zr alloys was higher than both Ti and Ti-6Al-4V (Ref 68).

Biswas et al. have examined the biocompatibility and corrosion performance of laser nitrided Ti-6Al-4V and stated that laser nitriding is not changing the E_{corr} considerably. They also mentioned that it occurred due to the presence of a considerably large volume fraction of TiN in the microstructure and the interface between the TiN and α-Ti, leading to the formation of pits (Ref 69). Further, Yilbas et al. have also reported that, as TiN is an electrical conductor and electrochemically more stable than Ti-6Al-4V when substrates are galvanically connected with TiN which are exposed to an aggressive electrolytes through these channels, the exposed regions will start to dissolve anodically. In addition, the small anodic area through the pinholes will lead to a local increase in current density and hence fasten the corrosion process at these points as channels for the corrosion of the substrate, which in

Table 2 Summary of the treated and untreated (in italics) samples properties calculated from the nanoindentation tests

Sample	H, GPa	E_r, GPa	H^3/E_r^2, GPa	Reference
Untreated alloy	*7.62*	*129*	*0.0269*	*Present study*
Treated alloy	*13.68*	*199.7*	*0.075*	*Present study*
Ti-6Al-4V (untreated)	5.0	121	0.009	(Ref 36)
Ti-6Al-4V (untreated)	NA	114	NA	(Ref 32)
Ti-6Al-4V (treated)		177		
Ti-35Nb7.3Zr5.7Ta (untreated)	4.8	63.8	0.027	(Ref 26)
Ti-35Nb7.3Zr5.7Ta (treated)	14.3	171.2	0.101	(Ref 26)

Table 3 Tafel parameters of the as-received and nitrided samples in SBF

Sample	E_{corr}, mV	i_{corr}, μA cm^2 × 10^{-3}	β_a, mV/dec	β_C, mV/dec	Corr. Rate, mpy × 10^{-3}
CpTi	−372	40.4	39	26	35.70
Ti6Al4V	−369	30.4	53	66	26.76
Untreated TNZ	−314	15.84	88	74	13.70
Treated TNZ	1.80	0.45	80	83	0.04

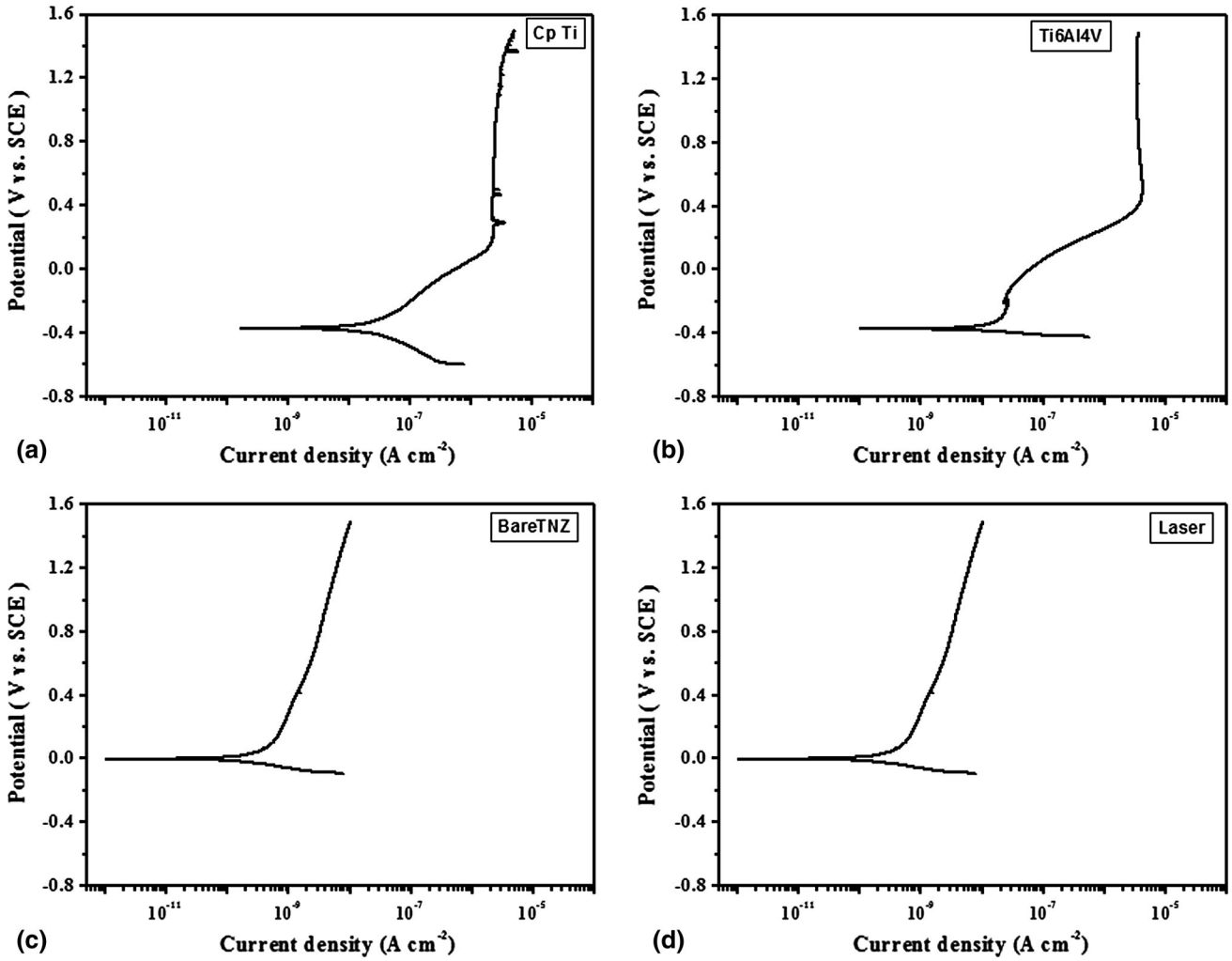

Fig. 5 Potentiodynamic polarization curves of (a) CpTi, (b) Ti6Al4V, (c) bare TNZ, and (d) laser-treated TNZ

turn effects in flaking of the nitrided layer (Ref 35). However, the E_{corr} of laser-treated TNZ in the present investigation is shifted in nobler direction than that of the investigated substrates, indicating an improved corrosion protection performance, which is ascribed to the production of compact and dense TiN layer with the fine-grained structure and the corrosion inhibition offered to Ti atoms from leaching, which correspond well with previous reports (Ref 40, 60). Man et al.

have reviewed the advantages of laser nitriding process on Ti alloys and mentioned that attention must be carefully engaged when treating the surface with laser beams since surface cracking reduces the fatigue life and corrosion resistance of the components (Ref 70). However, in the present study, the surface microstructure of the laser nitriding is clearly observed with no cracks and pores and confirmed the dense and compact surface with micro-/nanograins, which further confirmed the enhanced corrosion resistance. Furthermore, laser treatment can increase the corrosion protection performance of the TNZ alloys in SBF medium.

The EIS results are presented in Nyquist format in Fig. 6 which plots the real (Z') and imaginary (Z'') components of the impedance on x and y axes, respectively. Bare substrates (CpTi, Ti6Al4V, and TNZ) exhibit one capacitive arc, demonstrating a charge transfer process above a double layer, whereas the Nyquist plot obtained for the laser-treated TNZ substrates can be clearly distinguished as two separate capacitive arcs (see the inset in Fig. 6), signifying a charge transfer reaction over the TNZ surface that comprises two capacitances from different origins. In addition, the length of the first capacitive arc is smaller compared to that of the low-frequency capacitive arc, which is close to 10^7 Ω cm^2. A capacitive arc with a larger diameter indicates a higher corrosion resistance.

In general, EIS data in Nyquist plot show that the frequency decrease from left to right as the graph is not showing the frequency for data observed; thus, the similar data are frequently also exhibited by Bode plot displaying the relation between the frequency (f) with phase angle(θ) and the equivalent impedance (Z) as shown in Fig. 7, which displays the Bode plots of the bare and laser-treated TNZ alloy substrates. All the investigated Ti alloys exhibited the highly capacitive behavior, as specified by the mid to low frequencies with phase angles nearing −80°, signifying that a highly stable layer is produced over investigated alloys in the SBF. Based on the changes in the number of the phase angle, the bare substrates display only one well-defined time constant at a frequency of approximately 10 Hz, which is attributed to the controlled charge transfer reaction. By contrast, laser-treated TNZ alloys exhibit two relaxation time constants at frequencies of 10,000 and 10 Hz (similar to the frequency observed on the bare substrates). The existence of the time constant at a higher-frequency region is attributed to the laser-treated surface, signifying that it has a strong physical barrier against the aggressive environment. In general, the total impedance modulus ($|Z|$) for the low-frequency area in the EIS plots signifies the barrier performance of the coatings (Ref 71, 72). The different behavior of the laser-treated TNZ is associated with the elimination of TiO_2 layer and the existence of a TiN layer with chemically inert behavior. A maximum impedance value among the investigated alloys is attained for the laser-treated TNZ alloys, demonstrating the significant enhancement in the corrosion resistance of TNZ alloys with laser treatment.

Quantitative analysis of EIS data involves the equivalent circuit fitting analysis by selecting the appropriate equivalent circuit models. In the present investigation, two different equivalent circuit models (Fig. 8a, b) were employed to fit the EIS spectra of the bare and treated TNZ substrates using Echem software. Several researchers have proposed similar equivalent circuits (Ref 73-75). The capacitance was replaced by a constant phase element (CPE/Q) corresponding to the deviance from the perfect dielectric behavior and the surface hetero-

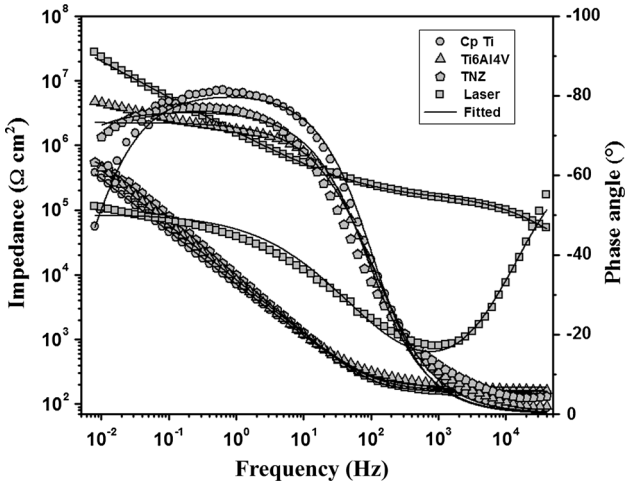

Fig. 7 Bode plots of the as-received and nitrided samples in SBF

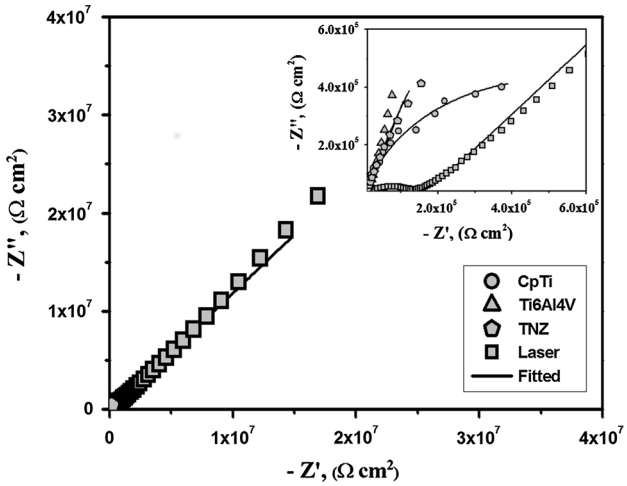

Fig. 6 Nyquist plots of the as-received and nitrided samples in SBF

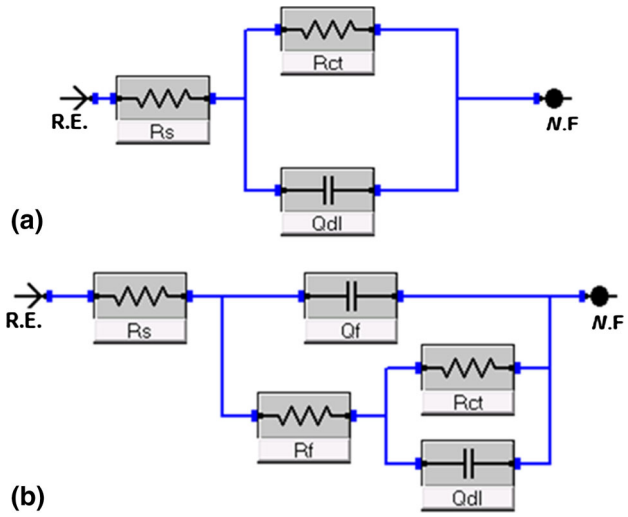

Fig. 8 EIS circuits models of: (a) the as-received and (b) the nitrided alloys

Table 4 EIS parameters of the as-received and nitrided samples in SBF

Sample	R_s, Ω cm^2	Q_{dl}, μF cm^{-2}	n_{dl}	R_f, kΩ cm^2	Q_f, μF cm^{-2}	n_f	R_{ct}, kΩ cm^2
CpTi	154	31.25	89	…	…	…	394
Ti6Al4V	146	25.10	81	…	…	…	435
Untreated TNZ	169	19.26	84	…	…	…	556
Treated TNZ	172	0.23	95	153.4	0.12	89	29.12×10^3

geneity to obtain the optimal fitting (Ref 76, 77). The EIS circuit models include the electrolytic resistance (R_s), film resistance (R_f), charge transfer resistance (R_{ct}), and constant phase element (CPE) of the film capacitance Q_f and double-layer capacitance Q_{dl}. Further, the quality of the fitting analysis can be estimated using the Chi-squared (χ^2) parameter, which is in the range of 10^{-4} and the obtained values revealed that the fitted results were consistent with the experimental results.

The EIS parameters shown in Table 4 were obtained using fitting analysis of the EIS results through the equivalent circuit model. The laser-treated TNZ substrates exhibited good barrier performance, with a film resistance R_f of 153 kΩ cm^2 and a high R_{ct} value of 29.12×10^3 kΩ cm^2 (versus 435 kΩ cm^2 for bare TNZ). Furthermore, the laser-treated substrates exhibited a decrease in CPE_{dl} by three orders of magnitude, which indicates a considerable reduction in the penetration of aggressive species from the harsh environment (Ref 78). It has been already reported that the chemical inertia of TiN surface greatly improves the material's surface protection against corrosion based on an investigation of corrosion behavior in harsh environments (Ref 59). Hence, the significant benefits of laser-treated TNZ alloys over bare and commercial alloys in terms of electrochemical corrosion performance were reflected in the larger capacitive loops and higher R_{ct} with lower Q_{dl} values and more positive E_{corr} with lower i_{corr} values, thus revealing the efficiency and solidness of the compact laser nitride surface in improving the corrosion resistance of TNZ alloys.

4. Conclusion

In this study, laser gas nitriding was performed using a CO2 laser (LC-ALPHAIII) to enhance the corrosion and surface characteristics of newly developed Ti-20Nb-13Zr at.% alloy. The treated and untreated alloys were characterized using XRD and FE-SEM. Nanoindentation and electrochemical investigations were performed to assess the surface and corrosion protection behavior of the untreated and nitrided samples. The following conclusion can be drawn:

1. The laser nitriding of the newly developed Ti20Nb13Zr showed the formation of TiN film on the alloy surface with micro-/nanograin size and 9.1 μm below the surface.
2. The nanoindentation results show the improvements in the hardness, modulus of elasticity, and resistance to plastic deformation of the alloy surface, thus indicating the alloy's higher resistance to wear.
3. The corrosion results indicated an enhancement in the corrosion resistance of laser-treated Ti20Nb13Zr alloys compared to as-received and commercial titanium and Ti6Al4V alloys.
4. The results also showed that laser treatment could be suggested for improving the surface hardness and corrosion protection characteristics of Ti-based alloys for biomedical fields.

Acknowledgments

The authors wish to acknowledge financial funding delivered by King Fahd University of Petroleum and Minerals, Project No. #IN151013.

References

1. J. Probst, U. Gbureck, and R. Thull, Binary Nitride and Oxynitride PVD Coatings on Titanium for Biomedical Applications, *Surf. Coat. Technol.*, 2001, **2**(148), p 226–233
2. A. Biesiekierski, J. Wang, M. Abdel-Hady Gepreel, and C. Wen, A New Look at Biomedical Ti-Based Shape Memory Alloys, *Acta Biomater.*, 2012, **8**(5), p 1661–1669
3. M.O. Alam and A.S.M.A. Haseeb, Response of Ti-6Al-4V and Ti-24Al-11Nb Alloys to Dry Sliding Wear Against Hardened Steel, *Tribol. Int.*, 2002, **35**(6), p 357–362
4. M.A. Hussein, A.S. Mohammed, and N. Al-Aqeeli, Wear Characteristics of Metallic Biomaterials: A Review, *Materials*, 2015, **8**(5), p 2749–2768
5. P.G. Liang, A. Ferguson, and E.S. Hodge, Tissue Reaction in Rabbit Muscle Exposed to Metallic Implants, *J. Biomed. Mater. Res.*, 1967, **1**(1), p 135–149
6. M.A. Khan, R.L. Williams, and D.F. Williams, In-vitro Corrosion and Wear of Titanium Alloys in the Biological Environment, *Biomaterials*, 1996, **17**(22), p 2117–2126
7. M. Chellappa and U. Vijayalakshmi, Electrophoretic Deposition of Silica and its Composite Coatings on Ti-6Al-4V, and Its In Vitro Corrosion Behaviour for Biomedical Applications, *Mater. Sci. Eng: C*, 2017, **71**, p 879–890
8. C.H. Ng, N. Rao, W.C. Law, G. Xu, T.L. Cheung, F.T. Cheng, X. Wang, and H.C. Man, Enhancing the Cell Proliferation Performance of NiTi Substrate by Laser Diffusion Nitriding, *Surf. Coat. Technol*, 2017, **309**, p 59–66
9. X. Liu, P.K. Chu, and C. Ding, Surface Modification of Titanium, Titanium Alloys, and Related Materials for Biomedical Applications, *Mater. Sci. Eng. R Rep*, 2004, **47**(3), p 49–121
10. Z.A. Uwais, M.A. Hussein, M.A. Samad, and N. Al-Aqeeli, Surface Modification of Metallic Biomaterials for Better Tribological Properties: A Review, Arab J. Sci. Eng., (2017). doi: 10.1007/s13369-017-2624-x
11. F.J. Braga, R.F. Marques, E.A. de Filho, and A.C. Guastaldi, Surface Modification of Ti Dental Implants by Nd: YVO 4 Laser Irradiation, *Appl. Surf. Sci.*, 2007, **253**(23), p 9203–9208
12. Y. Gao et al., Improved Biological Performance of Low Modulus Ti-24Nb-4Zr-7.9 Sn Implants Due to Surface Modification by Anodic Oxidation, *Appl. Surf. Sci*, 2009, **255**(9), p 5009–5015
13. R. Singh and N.B. Dahotre, Corrosion Degradation and Prevention by Surface Modification of Biometallic Materials, *J. Mater. Sci. Mater. Med.*, 2007, **18**(5), p 725–751
14. A. Kurella and N.B. Dahotre, Surface modification for Bioimplants: The Role of Laser Surface Engineering, *J. Biomater. Appl.*, 2005, **20**(1), p 5–50

15. S.T. Picraux and L.E. Pope, Tailored Surface Modification by Ion Implantation and Laser Treatment, *Science*, 1984, **226**, p 615–622
16. H. Zhou, F. Li, B. He, J. Wang, and B. Sun, Air plasma Sprayed Thermal Barrier Coatings on Titanium Alloy Substrates, *Surf. Coat. Technol.*, 2007, **201**(16), p 7360–7367
17. H. Gruner, Thermal Spray Coatings on Titanium, *Titan. Med. Springer*, 2001, **2001**, p 375–416
18. M. Ikeyama, S. Nakao, H. Morikawa, Y. Yokogawa, L.S. Wielunski, R.A. Clissold, and T. Bell, Increase of Surface Hardness Induced by O, Ca or P Ion Implantation into Titanium, *Surf. Coat. Technol.*, 2000, **128**, p 400–403
19. M. Tlotleng, E. Akinlabi, M. Shukla, and S. Pityana, Microstructures, Hardness and Bioactivity of Hydroxyapatite Coatings Deposited by Direct Laser Melting Process, *Mater. Sci. Eng. C*, 2014, **43**, p 189–198
20. M. Kaczmarek, M.U. Jurczyk, A. Miklaszewski, A. Paszel-Jaworska, A. Romaniuk, N. Lipińska, J. Żurawski, P. Urbaniak, and K. Jurczyk, In Vitro Biocompatibility of Titanium After Plasma Surface Alloying with Boron, *Mater. Sci. Eng. C*, 2016, **69**, p 1240–1247
21. G.C. Xu, Y. Hibino, Y. Nishimura, and M. Yatsuzuka, Hydrogenated Amorphous Carbon Formation with Plasma-Immersion Ion Plating, *Surf. Coat. Technol.*, 2003, **169**, p 299–302
22. H. Watanabe, Y. Sato, C. Nie, A. Ando, S. Ohtani, and N. Iwamoto, The Mechanical Properties and Microstructure of Ti-Si-N Nanocomposite Films by Ion Plating, *Surf. Coat. Technol.*, 2003, **169**, p 452–455
23. T. Matsue, T. Hanabusa, and Y. Ikeuchi, The Structure of TiN Films Deposited by Arc Ion Plating, *Vacuum*, 2002, **66**(3), p 435–439
24. K.G. Budinski, Tribological Properties of Titanium Alloys, *Wear*, 1991, **151**(2), p 203–217
25. V. Fouquet, L. Pichon, M. Drouet, and A. Straboni, Plasma Assisted Nitridation of Ti-6Al-4V, *Appl. Surf. Sci.*, 2004, **221**(1), p 248–258
26. B. Januszewicz and L. Klimek, Nitriding of Titanium and Ti6Al4V Alloy in Ammonia Gas Under Low Pressure, *Mater. Sci. Technol.*, 2010, **26**(5), p 586–590
27. B.S. Yilbas, C. Karatas, O. Keles, I.Y. Usta, and M. Ahsan, CO_2 Laser Gas Assisted Nitriding of Ti-6Al-4V Alloy, *Appl. Surf. Sci.*, 2006, **252**(24), p 8557–8564
28. M. Geetha, U.K. Mudali, N.D. Pandey, R. Asokamani, and B. Raj, Microstructural and Corrosion Evaluation of Laser Surface Nitrided Ti-13Nb-13Zr Alloy, *Surf. Eng.*, 2004, **20**(1), p 68–74
29. H. Behrndt and A. Lunk, Biocompatibility of TiN Preclinical and Clinical Investigations, *Mater. Sci. Eng A*, 1991, **139**, p 58–60
30. S. Shimadaa, T.Y. Takadaa, and J. Tsujino, Deposition of TiN Films on Various Substrates from Alkoxide Solution by Plasma-Enhanced CVD, *Surf. Coat. Technol.*, 2005, **199**(1), p 72–76
31. A. Śliwa, J. Mikuła, K. Gołombek, T. Tański, W. Kwaśny, M. Bonek, and Z. Brytan, Prediction of the Properties of PVD/CVD Coatings with the Use of FEM Analysis, *Appl. Surf. Sci.*, 2016, **388**, p 281–287
32. A. Naghibi, K. Raeissi, and M.H. Fathi, Corrosion and Tribocorrosion Behavior of Ti/TiN PVD Coating on 316L Stainless Steel Substrate in Ringer's Solution, *Mater. Chem. Phys.*, 2014, **148**(3), p 614–623
33. T.M. Muraleedharan and E.I. Meletis, Surface Modification of Pure Titanium and Ti-6Al-4V by Intensified Plasma Ion Nitriding, *Thin Solid Films*, 1992, **221**(1–2), p 104–113
34. K.L. Dahm, I.A. Anderson, and P.A. Darnley, Hard Coatings for Orthopedic Implants, *Surf. Eng.*, 1995, **11**(2), p 138–144
35. B.S. Yilbas, A.Z. Sahin, Z. Ahmad, and B.J.A. Aleem, A Study of the Corrosion Properties of TiN Coated and Nitrided Ti-6Al-4V, *Corros. Sci.*, 1995, **37**(10), p 1627–1636
36. B.S. Yilbas, A.F. Arif, C. Karatas, S. Akhtar, and B.J. Aleem, Laser Nitriding of Tool Steel: Thermal Stress Analysis, *Int. J. Adv. Manuf. Technol.*, 2010, **49**(9), p 1009–1018
37. P. Jiang, X.L. He, X.X. Li, L.G. Yu, and H.M. Wang, Wear Resistance of a Laser Surface Alloyed Ti-6Al-4V Alloy, *Surf. Coat. Technol.*, 2000, **130**(1), p 24–28
38. I. Garcia and J.J. De Damborenea, Corrosion Properties of TiN Prepared by Laser Gas Alloying of Ti and Ti6Al4V, *Corros. Sci.*, 1998, **40**(8), p 1411–1419
39. T.M. Manhabosco, S.M. Tamborim, C.B. Dos Santos, and I.L. Müller, Tribological, Electrochemical and Tribo-Electrochemical Characterization of Bare and Nitrided Ti6Al4V in Simulated Body Fluid Solution, *Corros. Sci.*, 2001, **53**(5), p 1786–1793
40. S. Sathish, M. Geetha, N.D. Pandey, C. Richard, and R. Asokamani, Studies on the Corrosion and Wear Behavior of the Laser Nitrided Biomedical Titanium and Its Alloys, *Mater. Sci. Eng. C*, 2010, **30**(3), p 376–382
41. H.D. Vora, R.S. Rajamure, S.N. Dahotre, Y.H. Ho, R. Banerjee, and N.B. Dahotre, Integrated Experimental and Theoretical Approach for Corrosion and Wear Evaluation of Laser Surface Nitrided, Ti-6Al-4V Biomaterial in Physiological Solution, *J. Mech. Behav. Biomed. Mater.*, 2014, **37**, p 153–164
42. T.M. Manhabosco, S.M. Tamborim, C.B. dos Santos, and I.L. Müller, Tribological, Electrochemical and Tribo-Electrochemical Characterization of Bare and Nitrided Ti6Al4V in Simulated Body Fluid Solution, *Corros. Sci.*, 2011, **53**(5), p 1786–1793
43. M.A. Hussein, C. Suryanarayana, and N. Al-Aqeeli, Fabrication of Nano-grained Ti-Nb-Zr Biomaterials Using Spark Plasma Sintering, *Mater. Des.*, 2015, **78**, p 693–700
44. M.V. Popa, E. Vasilescu, P. Drob, C. Vasilescu, S.I. Drob, D. Mareci, and J.C.M. Rosca, Corrosion Resistance Improvement of Titanium Base Alloys, *Quim. Nova*, 2010, **33**(9), p 1892–1896
45. C.H. Ng, C.W. Chan, H.C. Man, D. Waugh, and J. Lawrence, Modifications of Surface Properties Of Beta Ti by Laser Gas Diffusion Nitriding, *J. Laser Appl.*, 2016, **28**(2), p 022505
46. W.C. Oliver and G.M. Pharr, An Improved Technique for Determining Hardness and Elastic Modulus Using Load and Displacement Sensing Indentation Experiments, *J. Mater. Res.*, 1992, **7**(6), p 1564–1583
47. T. Kokubo and H. Takadama, How Useful is SBF in Predicting In vivo Bone Bioactivity, *Biomaterials*, 2006, **27**(15), p 2907–2915
48. H.C. Man, M. Bai, and F.T. Cheng, Laser Diffusion Nitriding of Ti-6Al-4V for Improving Hardness and Wear Resistance, *Appl. Surf. Sci.*, 2011, **258**(1), p 436–441
49. B.S. Yilbas, H. Ali, and C. Karatas, Laser Gas Assisted Treatment of Ti-Alloy: Analysis of Surface Characteristics, *Opt. Laser Technol.*, 2016, **78**, p 159–166 ([INVITED])
50. S.L.R. Da Silva, L.O. Kerber, L. Amaral, and C.A. Dos Santos, X-ray Diffraction Measurements of Plasma-Nitrided Ti-6Al-4V, *Surf. Coat. Technol.*, 1999, **116**, p 342–346
51. A. Biswas, L. Li, U.K. Chatterjee, I. Manna, S.K. Pabi, and J.D. Majumdar, Mechanical and Electrochemical Properties of Laser Surface Nitrided Ti-6Al-4V, *Scr. Mater.*, 2008, **59**(2), p 239–242
52. E. Toeroek, A.J. Perry, L. Chollet, and W.D. Sproul, Young's Modulus of TiN, TiC, ZrN and HfN, *Thin Solid Films*, 1987, **153**(1–3), p 37–43
53. J.C. Caicedo, G. Zambrano, W. Aperador, L. Escobar-Alarcon, and E. Camps, Mechanical and Electrochemical Characterization of Vanadium Nitride (VN) Thin Films, *Appl. Surf. Sci.*, 2011, **258**(1), p p312–p320
54. G.S. Kim, S.Y. Lee, J.H. Hahn, and S.Y. Lee, Synthesis of CrNyAlN Superlattice Coatings Using Closed-Field Unbalanced Magnetron Sputtering Process, *Surf. Coat. Technol.*, 2003, **171**(1), p 91–95
55. A. Hynowska, A. Blanquer, E. Pellicer, J. Fornell, S. Suriñach, M. Baró, S. González, E. Ibáñez, L. Barrios, C. Nogués, and J. Sort, Novel Ti–Zr–Hf–Fe Nanostructured Alloy for Biomedical Applications, *Materials*, 2013, **11**(6), p 4930–4945
56. J.P. Hirth, The Influence of Grain Boundaries on Mechanical Properties, *Metall. Trans.*, 1972, **3**(10), p 3047–3067
57. L. Thair, U.K. Mudali, N. Bhuvaneswaran, K.G.M. Nair, R. Asokamani, and B. Raj, Nitrogen Ion Implantation and In Vitro Corrosion Behavior of as-cast Ti-6Al-7Nb Alloy, *Corros. Sci.*, 2002, **44**(11), p 2439–2457
58. E. Galvanetto, F.P. Galliano, A. Fossati, and F. Borgioli, Corrosion Resistance Properties of Plasma Nitrided Ti-6Al-4V Alloy in Hydrochloric Acid Solutions, *Corros. Sci.*, 2002, **44**(7), p 1593–1606
59. S. Rossi, L. Fedrizzi, T. Bacci, and G. Pradelli, Corrosion Behaviour of Glow Discharge Nitrided Titanium Alloys, *Corros. Sci.*, 2003, **45**(3), p 511–529
60. S.S. Latthe, P. Sudhagar, A. Devadoss, A.M. Kumar, S. Liu, C. Terashima, K. Nakata, and A. Fujishima, Mechanically Bendable Superhydrophobic Steel Surface with Its Self-cleaning and Corrosion-Resistant Properties, *J. Mater. Chem. A*, 2015, **3**(27), p 14263–14271
61. M. Geetha, D. Durgalaksshmi, and R. Asokamani, Biomedical Implants: Corrosion and its Prevention—A Review, *Recent Pat. Corros. Sci.*, 2010, **2**, p 40–54
62. H.J. Rack and J.I. Qazi, Titanium Alloys for Biomedical Applications, *Mat. Sci. Eng. C*, 2006, **26**(8), p 1269–1277
63. A. Choubey, B. Basu, and R. Balasubramaniam, Electrochemical Behavior of Ti-based Alloys in Simulated Human Body Fluid Environment, *Trends Biomater. Artif. Organs*, 2005, **18**(2), p 64–72

64. F.A. Shah, M. Trobos, P. Thomsen, and A. Palmquist, Commercially Pure Titanium (cp-Ti) Versus Titanium Alloy (Ti6Al4V) Materials as Bone Anchored Implants—Is One Truly Better Than the Other?, *Mater. Sci. Eng.: C*, 2016, **62**, p 960–966
65. J. Lu, Y. Zhao, H. Niu, Y. Zhang, Y. Du, W. Zhang, and W. Huo, Electrochemical Corrosion Behavior and Elasticity Properties of Ti-6Al-xFe Alloys for Biomedical Applications, *Mater. Sci. Eng C*, 2016, **62**, p 36–44
66. L. Chenghao, J. Li'nan, Y. Chuanjun, and H. Naibao, Crevice Corrosion Behavior of CP Ti, Ti-6Al-4V Alloy and Ti-Ni Shape Memory Alloy in Artificial Body Fluids, *Rare Metal Mater. Eng.*, 2015, **44**(4), p 781–785
67. I. Cvijović-Alagić, Z. Cvijović, S. Mitrović, V. Panić, and M. Rakin, Wear and Corrosion Behaviour of Ti-13Nb-13Zr and Ti-6Al-4V Alloys in Simulated Physiological Solution, *Corros. Sci.*, 2011, **53**(2), p 796–808
68. A. Robin, O.A.S. Carvalho, S.G. Schneider, and S. Schneider, Corrosion Behavior of Ti-xNb-13Zr Alloys in Ringer's Solution, *Mater. Corros.*, 2008, **59**(12), p 929–933
69. A. Biswas, L. Li, T.K. Maity, U.K. Chatterjee, B.L. Mordike, I. Manna, and J.D. Majumdar, Laser Surface Treatment of Ti-6Al-4V for Bio-implant Application, *Lasers Eng*, 2007, **17**(1–2), p 59–73
70. R.S. Razavi, G.R. Gordani, and H.C. Man, A Review of the Corrosion of Laser Nitrided Ti-6Al-4V, *Anti Corros. Methods Mater.*, 2011, **58**(3), p 140–154
71. R. Vera et al., Corrosion Protection of Carbon Steel and Copper by Polyaniline and Poly (ortho-methoxyaniline) Films in Sodium Chloride Medium. Electrochemical and Morphological Study, *J. Appl. Electrochem.*, 2007, **37**(4), p 19–525
72. M. Mobin and N. Tanveer, Corrosion Performance of Chemically Synthesized Poly(aniline-coo-toluidine) Copolymer Coating on Mild Steel, *J. Coat. Technol. Res.*, 2012, **9**(1), p 27–38
73. Y. Mantani and M. Tajima, Phase Transformation of Quenched α″ Martensite by Aging in Ti-Nb Alloys, *Mater. Sci. Eng.*, 2006, **438**(440), p 315–319
74. S.L. Assis, S. Wolynec, and I. Costa, Corrosion Characterization of Titanium Alloys by Electrochemical Techniques, *Electrochim. Acta*, 2006, **51**(8), p 1815–1819
75. D.Q. Martins, W.R. Osorio, M.E.P. Souza, R. Caram, and A. Garcia, Effects of Zr Content on Microstructure and Corrosion Resistance of Ti-30Nb-Zr Casting Alloys for Biomedical Applications, *Electrochim. Acta*, 2008, **53**(6), p 2809–2817
76. E. Salahinejad, M.J. Hadianfard, D.D. Macdonald, S. Sharifi-Asl, M. Mozafari, K.J. Walker, A. Tahmasbi Rad, S.V. Madihally, D. Vashaee, and L. Tayebi, Surface Modification of Stainless Steel Orthopedic Implants by sol–gel ZrTiO4 and ZrTiO4-PMMA Coatings, *J. Biomed. Nanotechnol.*, 2013, **9**(8), p 1327–1335
77. E. Salahinejad, M.J. Hadianfard, D.D. Macdonald, S. Sharifi-Asl, M. Mozafari, K.J. Walker, A. Tahmasbi Rad, S.V. Madihally, and L. Tayebi, In Vitro Electrochemical Corrosion and Cell Viability Studies on Nickel-Free Stainless Steel Orthopedic Implants, *PLoS One*, 2013, **8**(4), p 1–8
78. D. Pech, P. Steyer, A.-S. Loir, J.C. Sánchez-López, and J.-P. Millet, Analysis of the Corrosion Protective Ability of PACVD Silica-Based Coatings Deposited on Steel, *Surf. Coat. Technol.*, 2006, **201**(1), p 347–352